  Bull. Chem. Soc. Jpn., 57, 395—404 (1984)

Five-coordinate Bis(1,1,1,5,5,5-hexafluoro-2,4-pentanedionato)(tertiary phosphine)palladium(II) and -platinum(II) Complexes. X-Ray Crystal and Molecular Structures and Fluxional Motions in Solution

Seichi Okeya,*,† Toshiko Miyamoto, Shun'ichiro Ooi,* Yukio Nakamura, and Shinichi Kawaguchi*

Faculty of Science, Osaka City University, Sumiyoshi-ku, Osaka 558

†*Faculty of Education, Wakayama University, Fukiage, Wakayama 640*

(Received July, 29, 1983)

Five-coordinate complexes [M(hfac)$_2$L] (M=Pd, Pt; hfac=1,1,1,5,5,5-hexafluoro-2,4-pentanedionate anion) were produced by the reactions of [M(hfac)$_2$] with equimolar amounts of tertiary phosphines, phosphites, and triphenylarsine. They were characterized by ^{1}H, ^{13}C, ^{19}F, and ^{31}P NMR spectra in solution and several complexes containing bulky phosphines as L were isolated, and structures of [Pd(hfac)$_2${P(*o*-tolyl)$_3$}] and [Pt(hfac)$_2${P(cyclohexyl)$_3$}] were determined by X-ray analysis. Both complexes have very distorted square-pyramidal structures, one of the two hfac anions in either of them spanning the apical and basal coordination sites. NMR spectra at various temperatures disclosed the fluxional behaviors of these complexes which retain the solid-state structures at such low temperatures as −60 °C. Two kinds of twist mechanisms were proposed.

By our extensive studies, the ligand substitution reactions of bis(β-diketonato)palladium(II) and -platinum(II) with various nitrogen bases[1] and tertiary phosphines[2] were found to afford many types of complexes depending on the natures of the central metals, β-diketonate ligands, attacking Lewis bases, and solvents employed. In either case, a molecule of Lewis base L was considered to transform one of the chelating β-diketonate ligands (β-dik) into the *O*-unidentate state (β-dik-*O*) in the first stage of the overall reaction (Eq. 1). In fact several palladium(II) and

$$[M(\beta\text{-dik})_2]+L \longrightarrow [M(\beta\text{-dik})(\beta\text{-dik-}O)L] \quad (1)$$

platinum(II) complexes containing an *O*-unidentate 1,1,1-trifluoro-2,4-pentanedionate (tfac) ligand were isolated.[2]

The ligand substitution reactions of square-planar complexes usually proceed according to the associative mechanism[3] but the five-coordinate intermediate can hardly be detected experimentally,[4] although rather many stable five-coordinate palladium(II) and platinum(II) complexes have been prepared (*vide infra*). When the reaction between [Pd(tfac)$_2$] and tri-*o*-tolylphosphine was studied spectrophotometrically, a distinct isosbestic point was recorded, indicating that no intermediate was accumulated to an appreciable concentration.[5]

On the contrary, the reactions of bis(1,1,1,5,5,5-hexafluoro-2,4-pentanedionato)palladium(II) and -platinum(II) with bulky tertiary phosphines were found to give stable adducts [M(hfac)$_2$(PR$_3$)]. This paper reports the characterization of these five-coordinate complexes and their fluxional behaviors in solution as well as the molecular structures of two of them which were determined by the X-ray diffraction method.[6]

Experimental

Preparation of Compounds. The starting chelates [Pd(hfac)$_2$] and [Pt(hfac)$_2$] were prepared according to the previously reported method.[7] Commercially supplied tertiary phosphines were used without further purification except P(*o*-tolyl)$_3$ which was recrystallized from ethanol.

*Bis(1,1,1,5,5,5-hexafluoro-2,4-pentanedionato)(tri-o-tolylphosphine)palladium(II), [Pd(hfac)$_2${P(o-tolyl)$_3$}] (**1a**)*: After [Pd(hfac)$_2$] (494 mg, 0.949 mmol) and P(*o*-tolyl)$_3$ (293 mg, 0.963 mmol) were dissolved in hot hexane (10 cm^3), the mixture was kept at −5 °C in a refrigerator to precipitate dark red crystals, which were filtered, washed with a small amount of hexane, and dried *in vacuo* (530 mg). The filtrate was allowed to stand at room temperature to make the solvent evaporate spontaneously. Another crop of crystals was left on the wall of vessel. The combined yield was 669 mg (85%). Red plates obtained by recrystallization from hexane were subjected to X-ray analysis.

*Bis(1,1,1,5,5,5-hexafluoro-2,4-pentanedionato)(tri-o-tolylphosphine)platinum(II), [Pt(hfac)$_2${P(o-tolyl)$_3$}] (**2a**)*: A solution of [Pt(hfac)$_2$] (254 mg, 0.417 mmol) and P(*o*-tolyl)$_3$ (127 mg, 0.417 mmol) in diethyl ether (15 cm^3) was kept standing at ambient temperature to allow the solvent to vaporize spontaneously. Orange plates left on the wall of vessel were gathered, washed with a small amount of hexane, and dried *in vacuo*. The yield was 339 mg (89%).

*Bis(1,1,1,5,5,5-hexafluoro-2,4-pentanedionato)(phenyldi-o-tolylphosphine)palladium(II), [Pd(hfac)$_2${PPh(o-tolyl)$_2$}] (**1b**) and -platinum(II), [Pt(hfac)$_2${PPh(o-tolyl)$_2$}] (**2b**)*: Both compounds were prepared in a similar way and the yield was 70% in either case. Recrystallization from hexane gave red plates (**1b**) and yellow needles (**2b**), respectively.

*Bis(1,1,1,5,5,5-hexafluoro-2,4-pentanedionato)(tricyclohexylphosphine)platinum(II), [Pt(hfac)$_2$(PCy$_3$)] (**2g**)*: The complex was also prepared by the method similar to that for **2a** in a 93% yield. Orange columns obtained by recrystallization from hexane were used for X-ray analysis.

*(1,1,1,5,5,5-Hexafluoro-2,4-pentanedionato){2-(di-o-tolylphosphino)benzyl-C,P}palladium(II), [(hfac)PdCH$_2$(o-C$_6$H$_4$)P(o-tolyl)$_2$] (**3**)*: A solution of **1a** (350 mg, 0.424 mmol) in dichloromethane (5 cm^3) was left to stand at ambient temperature for 10 d and the solvent was then allowed to evaporate spontaneously to leave yellow oil. The crude product was dissolved in dichloromethane (0.5 cm^3). Petroleum ether (bp <60 °C) was added to the solution and the mixture was cooled to precipitate yellow plates, which were filtered and dried *in vacuo*. The yield was 124 mg (47%). When kept at ambient temperature for a long time, even the solid specimen of **1a** changed gradually to **3**. Anal. Found: C, 50.60; H, 3.40% M$^+$, 616 (^{106}Pd, 27%), 618 (^{108}Pd, 27%), 615 (^{105}Pd, 22%), and 614 (^{104}Pd, 11%). Calcd for $C_{26}H_{21}O_2PF_6Pd$: C, 50.63; H, 3.43%; M, 616.79. ^{1}H NMR in $CDCl_3$, δ(ppm from internal Me_4Si): 2.45 and 2.75 (6H, s, br, 2CH_3); 3.79 (2H, d,

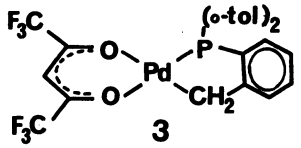

3

J(P-H)=4 Hz, CH_2); 6.8—7.3 (≈12H, ring protons). ^{13}C NMR in $CDCl_3$, δ(ppm from internal Me_4Si): 22.4 (d, br, ^3J(C-P)=10 Hz, ^1J(C-H)=*ca.* 130 Hz, CH_3); 32.1 (s, ^1J(C-H)=136 Hz, CH_2); 89.2 (s, br, ^1J(C-H)=164 Hz, CH of hfac). Other carbon signals are not analyzed. The ^{31}P NMR signal is observed in $CDCl_3$ as a singlet at 35.6 ppm downfield from external H_3PO_4. The above-mentioned splitting and broadening of methyl proton signals and broadening of methyl carbon signal seem to be caused by the restricted free rotation of the two tolyl groups around the P-C bonds. These signals became a broad singlet and a doublet, respectively at 50 °C.

X-Ray Analysis. The crystal data for [Pd(hfac)$_2${P(*o*-tolyl)$_3$}] (**1a**) and [Pt(hfac)$_2$(PCy$_3$)] (**2g**) are given in Table 1. The Laue symmetries and the space groups were determined from Weisenberg and precession photographs. The unit cell dimensions were obtained from the least-squares treatment of 20 θ values of higher angle reflections (θ=7—15 °) measured on an automated diffractometer by use of Mo$K\alpha$ radiation.

The intensities were measured on the diffractometer by using graphite-monochromated Mo$K\alpha$ radiation. The background was counted at each side of the scan range. The intensities of three standard reflections monitored every 4 h for each compound showed no appreciable variation during the data collection. The intensity data from compound **2g** were corrected for absorption.[8]

The crystal structures were solved by the heavy atom technique. The positional and thermal parameters were refined by block-diagonal-matrix least-squares. The minimized function was $\sum\omega(F_o-|F_c|)^2$, where $\omega=1/\sigma^2(F_o)$. All H atoms in **1a** could be found on the difference Fourier map but the refinement of their parameters was unsuccessful. They were included in the least-squares calculation but the parameters were fixed, the isotropic temperature factor $B_H=B+1.0$ being assigned for individual H atom, where B is the isotropic temperature factor of the C atom (obtained at the final cycle of isotropic refinement) to which the H atom is bound. No attempt was made to locate H atoms in **2g**. All parameter shifts in the final cycle of the refinement were less than 0.5σ in either case.

Table 1. Crystal data and experimental details

Compound	**1a**	**2g**
Crystal system	Monoclinic	Orthorhombic
Space group	$P2_1$	Pcab
a/Å	13.998(3)	25.652(3)
b/Å	11.430(2)	20.397(3)
c/Å	10.897(3)	12.781(2)
β/°	108.48(2)	
D_m/g cm^{-3}	1.66	1.75
D_c/g cm^{-3}	1.675	1.768
Z	2	8
μ(Mo $K\alpha$)/cm^{-1}	7.12	45.7
Crystal size/mm^3	0.18×0.20×0.27	0.15×0.22×0.30
Scan type	ω-2θ	ω
Scan speed (ω/s^{-1})	0.025	0.025
Scan range (ω/°)	1.0+0.3tanθ	0.8+0.4tanθ
Background count/s^{-1}	20	16
$2\theta_{max}$/°	55.0	50.0
No. of unique data ($F_o^2>3\sigma(F_o^2)$)	3148	3270
R	0.039	0.045
R'(=[$\sum\omega\Delta^2/\sum\omega F_o^2$]$^{1/2}$)	0.052	0.052

The atomic scattering factors, with correction for real part of anomalous dispersion of Pd^0 and Pt^0, were taken from Ref. 9. Compound **1a** crystallizes in a chiral space group, being resolved spontaneously on the way of crystallization. However, no attempt was made to determine the absolute crystal structure. The atomic coordinates are given in Table 2. The F_o—F_c tables, the anisotropic thermal parameters, and the H atom coordinates in **1a** are preserved at the Chemical Society of Japan (Document No. 8409). The computation was performed by a FACOM 230-60 computer at Osaka City University and ACOS-700 computer at Crystallographic Reserch Center of Osaka University by use of the program in the UNICS[10] and ORTEP.[11]

Other Measurements. Infrared spectra were obtained in Nujol mull with a Hitachi 295 spectrophotometer. Electronic spectra were measured in dichloromethane or hexane with a Hitachi 200-20 spectrophotometer. NMR spectra were recorded on JEOL-C60HL (in the case of ^1H), FX60Q (for ^1H, ^{13}C, and ^{31}P), FX90Q (for ^{13}C, ^{19}F, and ^{31}P), and FX100 (for ^{13}C and ^{195}Pt) instruments. A vapor-pressure osmometer manufactured by Knauer in West Berlin, West Germany, was used for molecular weight determination.

Results and Discussion

The reactions of [M(hfac)$_2$] (M=Pd^{II} and Pt^{II}) with equimolar amounts of bulky tertiary phosphines such as P(*o*-tolyl)$_3$ and PCy$_3$ in hexane or diethyl ether gave crystalline adducts [M(hfac)$_2$(PR$_3$)] (M=Pd (**1**) and Pt (**2**)) in high yields, of which decomposition temperatures and analytical data are listed in Table 3. Of these products, crystals of [Pd(hfac)$_2${P(*o*-tolyl)$_3$}] (**1a**) and [Pt(hfac)$_2$(PCy$_3$)] (**2g**) were suitable for X-ray analysis.

Molecular Structures in Crystals. Both crystals are composed of discrete complex molecules. Figures 1 and 2 show their perspective views and projections along the normal of the coordination plane for each molecule, respectively. Figure 3 gives the views of the phosphine ligands along the respective M-P vectors. As both complexes have similar ligands, common atom numbering is used as is seen in these Figures. Bond lengths and bond angles are summarized in Tables 4 and 5, respectively. Average values are given for the parameters of CF_3 groups, since these groups have large thermal parameters indicative of a disorder (Table 2) and hence individual structural parameter is of less importance.

The metal atom in either complex is five-coordinate and has a very distorted square-pyramidal coordination. The apical atom [O(11)] largely deviates from the ideal site for tetragonal symmetry as is seen in Fig. 2. The M-O(11) bond intersects the basal coordination plane defined by the O(12), O(21), O(22), and P atoms at 65.3(2)° and 66.9(3)° in **1a** and **2g**, respectively. The apical M-O bond is much longer than the basal one, indicating the weaker interaction between M and the apical O in either case. The basal donor atoms show slight but significant deviations from the mean plane, being displaced toward tetrahedral disposition. The magnitude is more than three times larger in **2g** than in **1a**. Although the O(12)-Pt-O(22) angle is 178.6(3)°, the P-Pt-O(21) angle is 173.1(2)° and the P and O(21) atoms are distant from the idealized apical site.

Such a very flattened tetrahedral arrangement of the

basal atoms has also been found in the pseudo tetragonal five-coordinate Pd^{II} and Pt^{II} complexes such as [MBr$_2$L$_3$] (M=Pd and Pt, L=5-ethyl(or methyl)-5*H*-dibenzophosphole;[12] M=Pd, L=2-phenylisophosphindoline[13]), [PdCl$_2$(PMe$_2$Ph)$_3$],[14] [PtCN(phen)$_2$]NO$_3$,[15] [Pd(hfac)(triphos)](hfac) (triphos =Ph$_2$PCH$_2$CH$_2$P(Ph)CH$_2$CH$_2$PPh$_2$),[16] and [Pd(hfac)$_2$(PPh$_3$)].[17] Furthermore, the metal atom is displaced from the basal plane toward the apical site, the deviation of Pd in **1a** being about twice as much as that of Pt in **2g**. Such deviation is characteristic of a square-pyramidal coordination of transition metals.

The Pt-P bond in **2g** is slightly but significantly shorter than Pd-P in **1a**. The M-O(21) bond, in which O(21) lies trans to the phosphine ligand, is somewhat longer than the other basal M-O bonds probably owing to the trans influence of the phosphine.

Table 2a. Fractional coordinates and temperature factors for [Pd(hfac)$_2${P(*o*-tolyl)$_3$}] (**1a**). Standard deviations of the least significant figures are given in parentheses

Atom	x	y	z	B_{eq}/Å^2
Pd	0.21720(3)	0.0 (1)	0.19120(4)	3.59(1)
O(11)	0.2992(5)	-0.1622(6)	0.3885(5)	6.4(2)
O(12)	0.2184(4)	-0.1499(5)	0.0941(5)	4.3(1)
C(11)	0.240(1)	-0.321(1)	0.4796(9)	7.8(4)
C(12)	0.2524(6)	-0.2525(7)	0.3628(7)	4.8(2)
C(13)	0.2025(6)	-0.3036(7)	0.2380(8)	5.1(3)
C(14)	0.1924(5)	-0.2501(6)	0.1214(7)	3.7(2)
C(15)	0.1420(7)	-0.3173(9)	0.0018(9)	6.0(3)
F(11)	0.268(1)	-0.2709(8)	0.5794(7)	17.5(6)
F(12)	0.2883(7)	-0.4190(7)	0.4949(8)	11.9(3)
F(13)	0.1441(7)	-0.360(1)	0.4537(9)	16.2(5)
F(14)	0.1912(5)	-0.3243(8)	-0.0784(6)	9.5(3)
F(15)	0.1149(7)	-0.4248(6)	0.0200(7)	11.4(3)
F(16)	0.0510(4)	-0.2632(8)	-0.0623(6)	9.9(3)
O(21)	0.0942(4)	-0.0631(5)	0.2401(5)	4.7(2)
O(22)	0.2015(4)	0.1566(5)	0.2645(5)	5.1(2)
C(21)	-0.0442(6)	-0.0662(9)	0.3146(9)	5.8(3)
C(22)	0.0447(4)	-0.001(1)	0.2923(6)	4.1(2)
C(23)	0.0589(6)	0.1159(7)	0.3282(7)	4.4(2)
C(24)	0.1336(5)	0.1836(7)	0.3099(6)	3.9(2)
C(25)	0.1376(7)	0.3121(8)	0.3465(8)	5.3(3)
F(21)	-0.0177(5)	-0.1673(6)	0.3690(7)	9.4(3)
F(22)	-0.1114(5)	-0.0944(7)	0.2058(7)	10.4(3)
F(23)	-0.0920(5)	-0.0077(9)	0.3772(8)	10.8(3)
F(24)	0.2083(7)	0.3298(7)	0.4532(7)	13.9(4)
F(25)	0.0550(6)	0.3523(6)	0.3611(8)	10.9(3)
F(26)	0.1564(6)	0.3791(5)	0.2607(7)	8.9(3)
P	0.3399(1)	0.0692(2)	0.1182(2)	3.30(5)
C(31)	0.3670(5)	0.2188(7)	0.1726(7)	3.8(2)
C(32)	0.4091(6)	0.2433(8)	0.3038(7)	4.8(2)
C(33)	0.4295(9)	0.360(1)	0.341(1)	7.4(4)
C(34)	0.4016(8)	0.4486(8)	0.248(1)	7.6(4)
C(35)	0.3611(7)	0.4253(8)	0.126(1)	6.4(3)
C(36)	0.3439(7)	0.3100(8)	0.0850(8)	5.1(3)
C(37)	0.4423(8)	0.149(1)	0.4091(8)	6.9(3)
C(41)	0.2936(5)	0.0604(7)	-0.0589(7)	3.9(2)
C(42)	0.1994(6)	0.0952(8)	-0.1299(7)	4.7(2)
C(43)	0.1725(7)	0.079(1)	-0.2650(8)	6.3(3)
C(44)	0.2361(7)	0.030(1)	-0.3230(7)	6.3(3)
C(45)	0.3242(6)	-0.008(1)	-0.2532(6)	5.6(2)
C(46)	0.3592(5)	0.009(1)	-0.1191(6)	4.5(2)
C(47)	0.1216(7)	0.144(1)	-0.0728(9)	7.0(3)
C(51)	0.4595(5)	-0.010(1)	0.1698(5)	4.0(2)
C(52)	0.5512(5)	0.0382(7)	0.1625(7)	4.5(2)
C(53)	0.6337(6)	-0.0304(9)	0.2035(8)	5.9(3)
C(54)	0.6300(7)	-0.145(1)	0.2493(8)	7.2(3)
C(55)	0.5446(6)	-0.1908(9)	0.2563(8)	5.5(3)
C(56)	0.4586(7)	-0.1233(8)	0.2168(8)	5.7(3)
C(57)	0.5616(6)	0.1563(9)	0.1097(9)	5.9(3)
H13	0.17500(0)	-0.37900(0)	0.23700(0)	6.00(0)
H23	0.01500(0)	0.15100(0)	0.36900(0)	5.00(0)
H33	0.46200(0)	0.37900(0)	0.43000(0)	7.50(0)
H34	0.41200(0)	0.52800(0)	0.27600(0)	7.70(0)
H35	0.34400(0)	0.48700(0)	0.06400(0)	7.10(0)
H36	0.31600(0)	0.29400(0)	-0.00500(0)	6.00(0)
H371	0.39300(0)	0.08900(0)	0.39400(0)	7.40(0)
H372	0.45000(0)	0.18300(0)	0.49200(0)	7.40(0)
H373	0.50400(0)	0.11800(0)	0.40700(0)	7.40(0)
H43	0.10700(0)	0.10200(0)	-0.31800(0)	7.20(0)
H44	0.21500(0)	0.02100(0)	-0.41400(0)	6.80(0)
H45	0.36600(0)	-0.04900(0)	-0.29300(0)	6.40(0)
H46	0.42600(0)	-0.01400(0)	-0.06900(0)	5.40(0)

Table 2b. Fractional coordinates and temperature factors for [Pt(hfac)$_2$(PCy$_3$)] (**2g**). Standard deviations of the least significant figures are given in parentheses

Atom	x	y	z	B_{eq}/Å^2
Pt	0.13785(2)	0.15649(2)	0.08025(3)	2.88(1)
O(11)	0.0337(3)	0.1391(4)	0.1309(9)	6.6(3)
O(12)	0.1408(3)	0.0592(3)	0.0861(6)	3.5(2)
C(11)	-0.0353(9)	0.077(1)	0.162(2)	16.(1)
C(12)	0.0215(5)	0.0826(7)	0.143(1)	4.9(4)
C(13)	0.0510(5)	0.0224(6)	0.128(1)	4.8(4)
C(14)	0.1044(5)	0.0184(6)	0.1062(9)	4.2(4)
C(15)	0.1284(5)	-0.0517(6)	0.108(1)	5.5(4)
F(11)	-0.0296(5)	0.0441(7)	0.275(1)	17.2(7)
F(12)	-0.0572(3)	0.0238(6)	0.1351(9)	11.4(4)
F(13)	-0.0574(4)	0.1184(6)	0.207(1)	16.2(6)
F(14)	0.1571(4)	-0.0623(4)	0.0275(8)	9.0(3)
F(15)	0.0939(4)	-0.0986(4)	0.1093(9)	11.3(4)
F(16)	0.1580(4)	-0.0585(4)	0.1931(7)	9.4(4)
O(21)	0.0944(3)	0.1473(3)	-0.0581(5)	4.0(2)
O(22)	0.1333(3)	0.2538(3)	0.0761(6)	4.0(2)
C(21)	0.0444(8)	0.1800(7)	-0.204(1)	9.0(7)
C(22)	0.0756(5)	0.1955(6)	-0.1036(9)	4.0(4)
C(23)	0.0789(5)	0.2634(5)	-0.0749(9)	4.1(3)
C(24)	0.1063(4)	0.2844(5)	0.0091(9)	3.5(3)
C(25)	0.1038(6)	0.3578(6)	0.035(1)	5.3(4)
F(21)	0.0209(6)	0.1270(6)	-0.1998(9)	16.6(6)
F(22)	0.0788(5)	0.1660(8)	-0.2763(8)	16.4(6)
F(23)	0.0191(5)	0.2239(5)	-0.2453(9)	13.7(5)
F(24)	0.0859(6)	0.3935(4)	-0.0382(8)	12.5(5)
F(25)	0.1498(3)	0.3813(4)	0.0593(9)	9.7(4)
F(26)	0.0743(5)	0.3682(4)	0.1141(8)	10.6(4)
P	0.1925(1)	0.1637(1)	0.2155(2)	3.0(1)
C(31)	0.2364(4)	0.0916(5)	0.2194(8)	3.7(3)
C(32)	0.2621(5)	0.0779(6)	0.1125(9)	4.5(4)
C(33)	0.2927(5)	0.0116(6)	0.119(1)	4.5(4)
C(34)	0.3315(5)	0.0102(6)	0.204(1)	5.1(4)
C(35)	0.3068(6)	0.0254(7)	0.312(1)	6.2(5)
C(36)	0.2784(5)	0.0947(7)	0.3093(9)	5.6(4)
C(41)	0.1589(4)	0.1654(6)	0.3422(8)	3.9(3)
C(42)	0.1290(5)	0.0994(6)	0.3606(9)	4.4(4)
C(43)	0.0960(5)	0.1035(8)	0.462(1)	6.1(5)
C(44)	0.0578(5)	0.1606(8)	0.461(1)	5.9(4)
C(45)	0.0880(6)	0.2251(7)	0.4483(9)	5.8(5)
C(46)	0.1205(5)	0.2256(7)	0.343(1)	4.9(4)
C(51)	0.2267(5)	0.2438(5)	0.2081(8)	3.5(3)
C(52)	0.2596(6)	0.2600(6)	0.307(1)	5.3(4)
C(53)	0.2843(6)	0.3317(6)	0.290(1)	6.1(5)
C(54)	0.3167(5)	0.3363(6)	0.193(1)	6.3(5)
C(55)	0.2853(6)	0.3169(6)	0.097(1)	6.2(5)
C(56)	0.2631(5)	0.2457(6)	0.1089(9)	4.8(4)

Table 3. Isolated five-coordinate complexes [M(hfac)$_2$(PR$_3$)]

Compd			Decomposition temp	Found (Calcd)		
No.	M	PR$_3$	°C	C(%)	H(%)	Mol wt[a]
1a	Pd	P(*o*-tolyl)$_3$	113—114	45.54(45.14)	2.86(2.81)	818(825)
2a	Pt	P(*o*-tolyl)$_3$	136—137	40.90(40.75)	2.52(2.54)	901(914)
1b	Pd	PPh(*o*-tolyl)$_2$	*ca.* 100	44.56(44.44)	2.68(2.61)	
2b	Pt	PPh(*o*-tolyl)$_2$	130—135	40.10(40.06)	2.39(2.35)	
2g	Pt	PCy$_3$[b]	128—133	37.86(37.80)	3.94(3.97)	814(890)

a) Determined in dichloromethane at 25 °C. b) PCy$_3$ abbreviates P(cyclohexyl)$_3$.

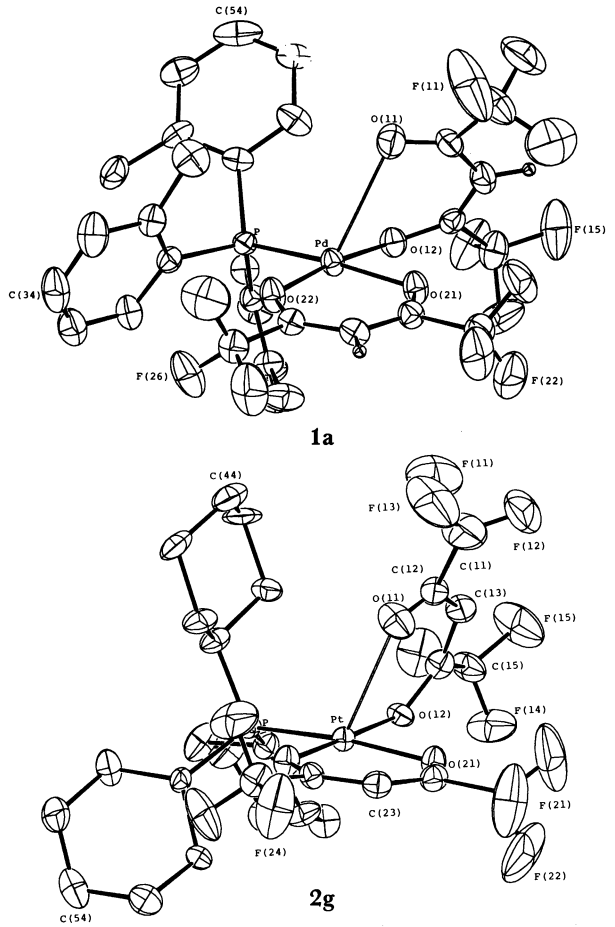

Fig. 1. ORTEP drawing of [Pd(hfac)$_2${P(*o*-tolyl)$_3$}] (**1a**) and [Pt(hfac)$_2$(PCy$_3$)] (**2g**). Thermal ellipsoids are drawn at 30% probability level. The H atom linked to the C(13) and C(23) atoms in **1a** are represented by spheres with arbitrary radius.

Table 4. Bond lengths

Bond length	*l*/Å	
	1a	**2g**
M–P	2.253(2)	2.232(3)
O(11)	2.796(6)	2.773(9)
O(12)	2.016(5)	1.988(6)
O(21)	2.086(6)	2.099(7)
O(22)	2.000(6)	1.990(7)
C(11)–C(12)	1.550(14)	1.48(3)
C(12)–O(11)	1.206(11)	1.203(16)
C(12)–C(13)	1.442(11)	1.455(18)
C(13)–C(14)	1.376(12)	1.399(17)
C(14)–O(12)	1.266(9)	1.275(14)
C(14)–C(15)	1.484(11)	1.557(16)
C(11), C(15)–F	1.302[a)]	1.34[a)]
C(21)–C(22)	1.537(13)	1.545(19)
C(22)–O(21)	1.251(11)	1.239(14)
C(22)–C(23)	1.384(14)	1.436(16)
C(23)–C(24)	1.366(11)	1.353(16)
C(24)–O(22)	1.242(10)	1.265(13)
C(24)–C(25)	1.519(12)	1.536(16)
C(21), C(25)–F	1.294[a)]	1.30[a)]
P–C(31)	1.810(8)	1.853(11)
C(41)	1.833(7)	1.835(11)
C(51)	1.830(8)	1.855(11)

a) Mean value of six C–F bond lengths.

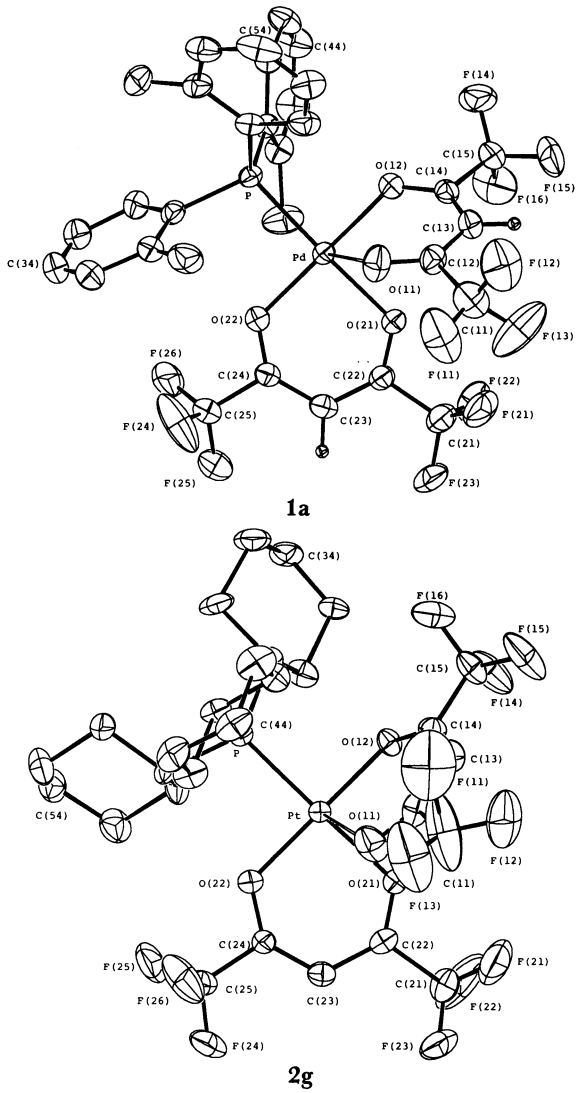

Fig. 2. Projection of each complex along the normal of coordination plane. Thermal ellipsoids are drawn at 30% probability level. The H atoms linked to the C(13) and C(23) atoms in **1a** are shown by spheres with arbitrary radius.

The hfac ligand lying on the basal plane in either complex forms a symmetrical planar chelate ring with the metal atom, and bond lengths indicate complete delocalization of π electrons within hfac. On the other hand, the hfac ligands which span the basal and apical sites in both complexes have structural parameters similar to each other. However, while the chelate ring in **2g** is totally planar, that in **1a** is folded along the line O(11)···O(12), the interplanar angle between the ligand plane (Plane 2 in Table 6) and the [Pd, O(11), O(12)] plane being 141.1(3)° as is seen in Fig. 2 and Table 6. Bond lengths clearly show the localization of π electrons in the latter ligand, indicating a greater contribution from the resonance structure $^{-}$O–C(CF$_3$)=CH–C(CF$_3$)=O. A detailed structural examination revealed that the two planar CF$_3$COC moieties are rotated with respect to each other through a dihedral angle of 9.2(4)°.

As stated already, the reactions of [M(tfac)$_2$] with bulky tertiary phosphines afford four-coordinate

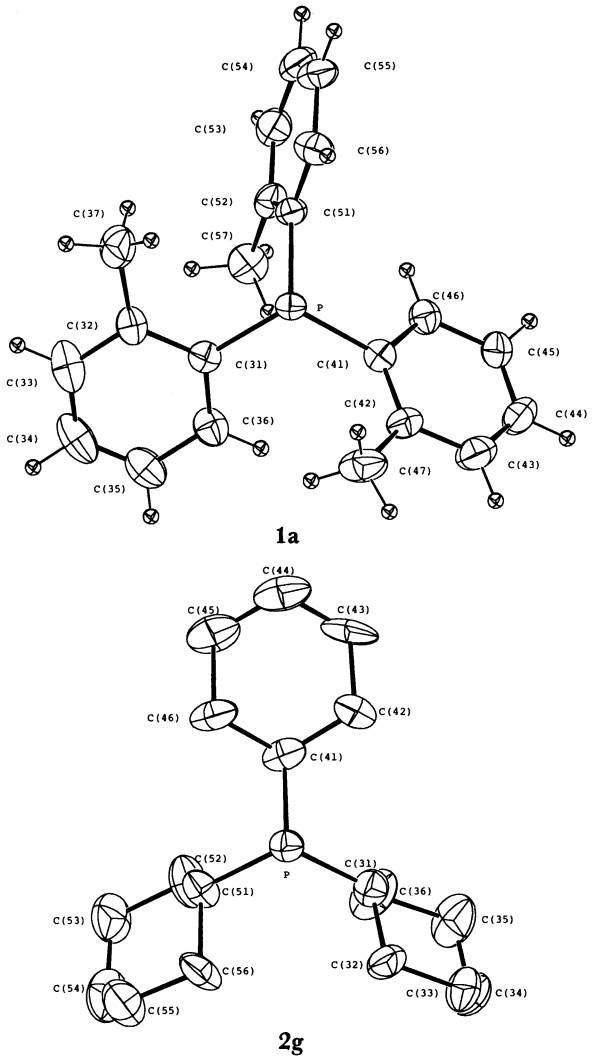

Fig. 3. The structures (30% ellipsoids) of the P(*o*-tolyl)$_3$ in **1a** and PCy$_3$ in **2g** viewed along the M–P vectors. Hydrogen atoms in **1a** are represented by spheres with arbitrary radius.

square-planar complexes [M(tfac)(tfac-*O*)(PR$_3$)] containing an *O*-unidentate tfac ligand, which is bound to the metal atom through the acetyl oxygen and the oxygen atom of the dangling trifluoroacetyl group is far from the metal atom, showing no sign of interaction.[18] On the other hand, an oxygen atom of hfac in [M(hfac)$_2$(PR$_3$)], which is obtained by a similar reaction, lies near the apical position of a square-pyramidal structure. The structural difference between these two types of complexes of similar composition may stem from (i) a greater net positive charge on the metal atom in the hypothetical complex [M(hfac)(hfac-*O*)(PR$_3$)] caused by the lower basicity of the hfac anion than that of tfac, and (ii) preference of the *Z,Z*-form by hfac over either *E,E*-, or *E,Z*-form because of repulsions between bulky CF$_3$ groups or between CF$_3$ and the carbonyl oxygen. Thus it seems reasonable that when an hfac anion is allowed to occupy a single basal site to link to a metal atom through one of the two oxygens, the other oxygen atom of the dangling CF$_3$CO group is positioned around the apical site. The lone-pair electrons of the apical donor atom can interact with a net positive charge on the metal which is effected by incomplete neutralization of the metal charge due to low basicities of σ donors and/or by back donation through the M-L π bonding, thus completing a five-coordination. It is worth noting that the reactions between [M(hfac)$_2$] and various nitrogen bases have never given rise to five-coordinate complexes.[1]

Table 5. Bond angles

Bond angle	ϕ/°	
	1a	**2g**
O(11)-M-O(12)	76.7(2)	84.2(3)
O(21)-M-O(22)	90.2(2)	92.0(3)
P-M-O(12)	88.8(2)	90.8(2)
P-M-O(22)	91.1(2)	89.5(2)
O(11)-M-O(21)	75.2(2)	70.9(3)
M-O(11)-C(12)	109.2(5)	113.7(8)
M-O(12)-C(14)	126.5(5)	129.1(7)
M-O(21)-C(22)	122.6(6)	122.2(7)
M-O(22)-C(24)	125.2(5)	122.8(7)
M-P-C(31)	108.7(3)	110.5(4)
M-P-C(41)	107.3(3)	112.9(4)
M-P-C(51)	116.3(3)	108.4(4)
C(11)-C(12)-C(13)	115.0(8)	118(1)
C(11)-C(12)-O(11)	115.9(7)	111(1)
C(13)-C(12)-O(11)	129.1(8)	131(1)
C(12)-C(13)-C(14)	124.7(8)	126(1)
C(13)-C(14)-O(12)	131.7(7)	136(1)
C(15)-C(14)-O(12)	110.7(7)	108(1)
C(15)-C(14)-C(13)	117.5(7)	116(1)
C(12)-C(11)-F C(14)-C(15)-F	112.6[a]	111[a]
F-C(11)-F F-C(15)-F	106[b]	102[b]
C(21)-C(22)-C(23)	118.4(8)	116(1)
C(21)-C(22)-O(21)	112.7(9)	116(1)
C(23)-C(22)-O(21)	128.9(8)	128(1)
C(22)-C(23)-C(24)	123.4(8)	123(1)
C(23)-C(24)-O(22)	129.5(7)	132(1)
C(25)-C(24)-O(22)	112.1(7)	111(1)
C(25)-C(24)-C(23)	118.4(8)	117(1)
C(22)-C(21)-F C(24)-C(25)-F	112.5[a]	113[a]
F-C(21)-F F-C(25)-F	106[b]	106[b]
C(31)-P-C(41)	111.4(3)	106.0(5)
C(31)-P-C(51)	107.0(4)	114.4(5)
C(41)-P-C(51)	106.3(3)	104.5(5)

a) Mean value of six C–C–F angles. b) Mean value of six F–C–F angles.

Structures and Dynamic Behaviors of the Five-coordinate Complexes in Solution. Electronic and Infrared Spectra: The electronic spectrum of complex **1a** exhibits absorption maxima at 302 nm (ε=18200) and 410 nm (ε=2500) in dichloromethane at room temperature, and shows no appreciable change in hexane at −90 °C, suggesting that the structure of **1a** in solution does not vary in this temperature range. The absorption maxima of **2a** in dichloromethane at room temperature were observed at 275 nm (ε=11600), 280 nm (ε=11500), and 308 nm (ε=9600).

On addition of increasing amounts of P(*o*-tolyl)$_3$ to a solution of [Pd(hfac)$_2$] in hexane, the absorption

Table 6. Atom deviation from mean plane and interplanar angle

	1a	
Atom deviation (d/Å)		
Plane 1	[O(12), O(21), O(22), P]	
	Pd, 0.122(2); O(12), −0.020(5); O(21), 0.021(5); O(22), −0.020(5); P, 0.019(3)	
Plane 2	[O(11), O(12), C(11), C(12), C(13), C(14), C(15)]	
	O(11), 0.094(9); O(12), −0.114(8); C(11), −0.104(15); C(12), 0.042(12); C(13), 0.043(12); C(14), −0.012(10); C(15), 0.050(11)	
Plane 3	[O(11), C(11), C(12), C(13)]	
	O(11), −0.005(7); C(11), −0.003(14); C(12), 0.013(11); C(13), −0.004(9)	
Plane 4	[O(12), C(13), C(14), C(15)]	
	O(12), −0.000(6); C(13), −0.000(9); C(14), 0.001(9); C(15), −0.000(10)	
Plane 5	[O(21), O(22), C(21), C(22), C(23), C(24), C(25)]	
	O(21), −0.027(6); O(22), 0.015(6); C(21), −0.008(9); C(22), 0.009(8); C(23), 0.033(9); C(24), 0.015(8); C(25), −0.035(9)	
Interplanar angle (φ/°)		
	[Pd, O(11), O(12)]-Plane 2	141.1(3)
	[Pd, O(21), O(22)]-Plane 5	177.2(5)
	Plane 3-Plane 4	9.2(4)
Tortion angle (τ/°)		
	O(11)-C(12)···C(14)-O(12)	6.8(8)

Table 6. (Continued)

	2g	
Atom deviation (d/Å)		
Plane 1	[O(12), O(21), O(22), P]	
	Pt, 0.052(3); O(12), 0.077(8); O(21), −0.078(8); O(22), 0.075(8); P, −0.073(4)	
Plane 2	[O(11), O(12), C(11), C(12), C(13), C(14), C(15)]	
	O(11), 0.029(13); O(12), −0.031(11); C(11), −0.025(26); C(12), 0.045(18); C(13), −0.044(18); C(14), −0.025(15); C(15), 0.050(16)	
Plane 3	[O(21), O(22), C(21), C(22), C(23), C(24), C(25)]	
	O(21), −0.049(10); O(22), 0.042(10); C(21), 0.026(20); C(22), −0.009(16); C(23), 0.008(17); C(24), 0.026(15); C(25), −0.045(16)	
Interplanar angle (φ/°)		
	[Pt, O(11), O(12)]-Plane 2	178.9(3)
	[Pt, O(21), O(22)]-Plane 3	175.2(4)

spectrum changed stepwisely, exhibiting distinct isosbestic points at 341 and 369 nm (Fig. 4). Addition of the phosphine beyond the equimolar amount caused no further change in spectrum and the final spectrum closely resembles that of the authentic sample of **1a**. These results clearly indicate that the reaction between [Pd(hfac)$_2$] and P(o-tolyl)$_3$ affords no product other than **1a** and that the equilibrium constant of this addition reaction is very large. As is shown in Table 3, the molecular weight data for complexes **1a**, **2a**, and **2g** in dichloromethane at room temperature nearly coincide with the calculated values, indicating that these complexes are stable in solution and do not dissociate the phosphine to any appreciable extent.

Infrared spectrum of **1a** includes characteristic bands at 1690(s), 1633(vs), 1550(vs), and 1530(s) cm^{-1} and **2a** also absorbs at 1705(m), 1616(s), 1564(vs), and 1523(m) cm^{-1}. In either case, the highest-frequency band may be assigned to the ν(C=O) vibration of the CF_3CO group occupying the apical position. The other bands lie in the frequency region which is related with the ν(C⋯O)+ν(C⋯C) vibrations of the usually O,O'-chelated hfac ligand.

^{1}H NMR Spectra: The ^{1}H NMR data for the isolated complexes listed in Table 3 are given in Table 7. The ^{1}H NMR signals observed for reaction mixtures of [Pd(hfac)$_2$] with equimolar amounts of various tertiary phosphines, arsines, and phosphites are also included in Table 7. The spectra are quite similar to those of **1a** and **2g**, suggesting that the reaction products probably have the five-coordinate structures

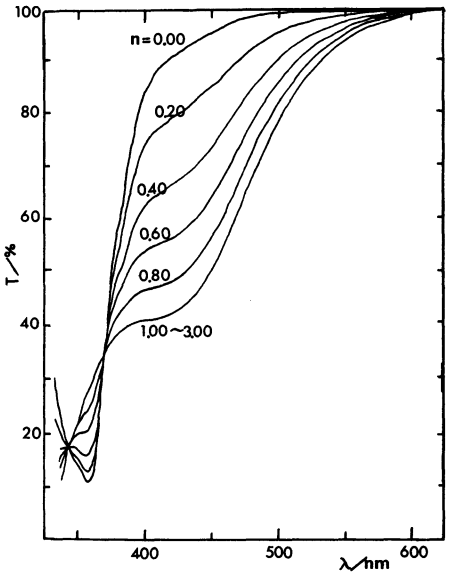

Fig. 4. Transmittance spectra of hexane solutions containing [Pd(hfac)$_2$] and n times molar amounts of P(o-tolyl)$_3$.
[complex]=1.50×10^{-4} mol dm^{-3}.

similar to those of **1a** and **2g**, although they were not isolated. Thus, in either case a single methine signal from the hfac ligands is observed at room temperature in the 5.8—6.1 ppm region except for **2i**, showing upfield shift by 0.3—0.6 ppm as compared with that from [M(hfac)$_2$]. Furthermore, the ^4J(Pt-H) values for the Pt^{II} complexes (**2**) are 5—7 Hz, about one half of 10.5 Hz for the parent bis-chelate, probably reflecting decrease in s-character of the platinum bonding with the change in structure from square to square-pyramid.

If the square-pyramidal structure in crystals is retained in solution, the two hfac ligands are not equivalent and should exhibit two methine proton

TABLE 7. ^{1}H NMR DATA FOR [M(hfac)$_2$L][a)]

Compd			Solvent	Temp	hfac-CH	L	
No.	M	L		°C		Me	Ph
1a	Pd	P(*o*-tolyl)$_3$	CD_2Cl_2	27	5.85	2.31	7.2—8.1c
			CD_2Cl_2	−50	6.15, 5.47	2.94, 2.10, 1.72	7.25br, 7.57br 9.27d, br((16))
2a	Pt	P(*o*-tolyl)$_3$	CD_2Cl_2	27	5.89{5}	2.27	7.2—7.7c
			CD_2Cl_2	−60	6.34, 5.31	2.74, 2.13, 1.69	7.2br, 7.5br, 9.15d, br((18))
1b	Pd	PPh(*o*-tolyl)$_2$	$CDCl_3$	27	5.88	2.47	7.2—8.1c
2b	Pt	PPh(*o*-tolyl)$_2$	CD_2Cl_2	27	5.92{5}	2.37	7.2—8.1c
1c	Pd	PPh_3	CD_2Cl_2	27	5.87		7.3—7.9br
2c	Pt	PPh_3	CD_2Cl_2	27	5.96{5}		7.3—7.9c
2d	Pt	$PMePh_2$	$CDCl_3$	27	5.97{6}	1.90d((12)){31}	7.3—7.9c
2e	Pt	PMe_2Ph	$CDCl_3$	27	6.06{7}	1.76d((13)){33}	7.4—7.9c
2f	Pt	PEt_3	$CDCl_3$	27	6.08{5}	Et: 1.0—2.0c	
1g	Pd	PCy_3	$CDCl_3$	27	5.97	Cy: 1.9br, 1.3br	
2g	Pt	PCy_3	$CDCl_3$	27	6.04{5}	Cy: 1.9br, 1.3br	
2h	Pt	P(OPh)$_3$	$CDCl_3$	27	5.97{6}		7.1—7.5c
2i	Pt	P(OEt)$_3$	$CDCl_3$	27	6.28{6}	Et: 4.29dq(7)((7)),	1.35dt(7)((2))
1j	Pd	$AsPh_3$	$CDCl_3$	27	5.90		7.54br
2j	Pt	$AsPh_3$	$CDCl_3$	27	5.96[b)]		7.54br

a) Chemical shifts in ppm from internal Me_4Si. Figures in parentheses, double parentheses, and braces are $^3J(CH_2$-$CH_3)$, J(P-H), and J(Pt-H) in Hz, respectively. d: Doublet, t: triplet, q: quartet, br: broad, c: complex. b) The ^{195}Pt satellites are indiscernible.

signals. In fact, at lower temperatures (−50 and −60 °C) either of complexes **1a** and **2a** shows two methine and three methyl signals, indicating that the stereochemically rigid five-coordinate structure is retained in solution at low temperatures. If free rotation of the phosphine ligand around the M-P bond is prohibited, the three methyl groups attached to the phenyl rings may have different environments from each other since there exists no plane of symmetry involving the M-P bond. Signals from the phenyl-ring protons also show splitting and a 1H doublet is observed for either of **1a** and **2a** at such a low field as 9.27 and 9.15 ppm, respectively. The α-proton of a phenyl ring attached to phosphorus might exist near the sixth coordination site around the metal and suffer its paramagnetic anisotropic effect. Although such a conformation is not reallized in the crystal of **1a**, the M···H-C interaction is rather frequently noticed in metal complexes[19] especially as a prerequisite for orthometallation.[20]

At room temperature, besides the free rotation of the phosphine ligand, the five-coordinate complex may undergo some fluxional motion to average environments of the two hfac ligands. In the case of complexes **1c** and **2c** containing triphenylphosphine probably as a basal ligand, the hfac-CH signal does not show splitting even at −50 °C. The smaller steric hindrance of PPh_3 than that of P(*o*-tolyl)$_3$ may enhance the stereochemical nonrigidity of the five-coordinate complex.

^{19}F NMR Spectra: Figure 5 shows the ^{19}F{^{1}H}NMR spectra of complexes **1a** and **2a** in CD_2Cl_2 at various temperatures. At −60 °C both complexes exhibit four signals at 73.8_3, 74.6_3, 75.7_1, and 76.5_4 ppm upfield from internal $CFCl_3$ in the case of **1a** and at 73.5_4, 74.3_9, 79.5_0, and 76.9_9 ppm upfield for **2a**. These spectra are consistent with the molecular structure of **1a** in the solid, indicating nonequivalence of the four CF_3 groups. The signals from **1a** become broad with increasing temperature, coalesce at around −40 °C and give rise to a sharp singlet at -75.8_5 ppm at 22 °C. On the other hand, complex **2a** exhibits a little different behavior. Two signals in the lower field merge at 22 °C to a sharp singlet at -74.4_2 ppm (half-height width=1.6 Hz) flanked by the ^{195}Pt satellites (J(Pt-F)= 15 Hz), whereas the remaining two signals in the

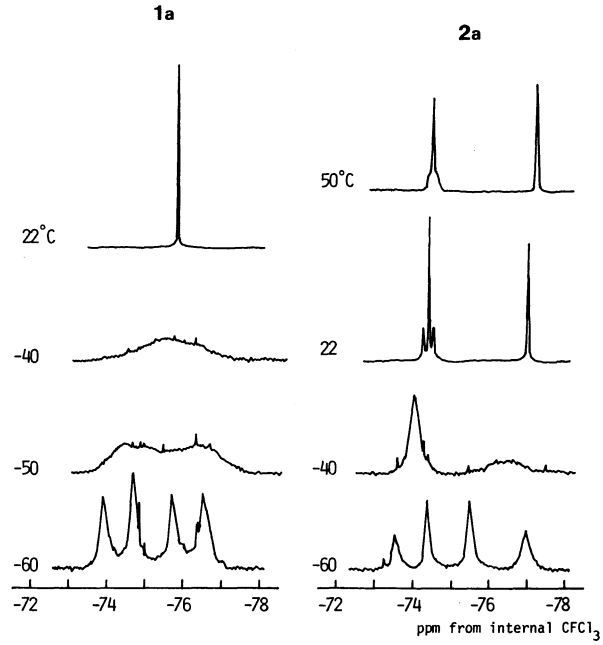

Fig. 5. ^{19}F{^{1}H} NMR spectra at 84.31 MHz of [Pd(hfac)$_2$-{P(*o*-tolyl)$_3$}] (**1a**) and [Pt(hfac)$_2${P(*o*-tolyl)$_3$}] (**2a**) in CD_2Cl_2 at several temperatures.

higher field are converted into a broader singlet at -77.0_1 ppm (half-height width=2.9 Hz). However, the two signals broaden at 50 °C, indicating that complex **2a** may behave in the same way as **1a** does but need much larger energy than **1a**.

Exchange between the basal and apical hfac ligands may be achieved by a twist motion via a trigonal-bipyramidal transition state as depicted in Eq. 1.

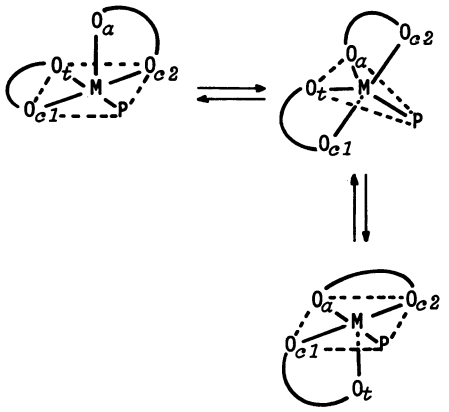

(1)

However, two halves of each hfac anion are not yet equivalent under this rapid motion. One half of each hfac is always near the site cis to phosphorus, while the other lies trans to P or at the apical site, being averaged. The ^1H and ^{19}F NMR spectra of complex **2a** at 22 °C are satisfactorily interpreted by this rapid intramolecular transformation (Eq. 1). Of the two ^{19}F signals, the lower-field one flanked by the ^{195}Pt satellites may be assigned to the CF_3 groups positioned cis to the phosphine, and the other broader high-field one to the average of CF_3 groups at the apical and trans sites, since the ^{19}F atoms around the positions cis to phosphine will couple to platinum more strongly than those around the apical and trans positions.

The ^{19}F NMR spectrum of **1a** at 22 °C can not be explained solely by Eq. 1, but needs another fluxional mode to average the cis and trans or apical positions. A simple oscillatory motion of the apical chelate ring as depicted in Eq. 2 may be sufficent to supplement mechanism (1) in averaging all four CF_3 groups.

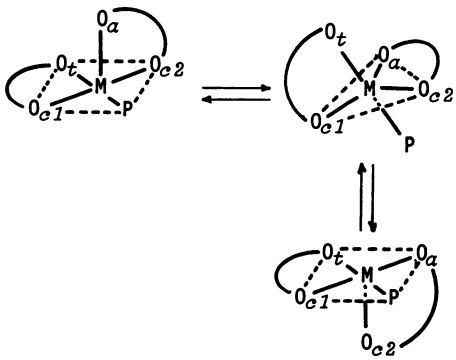

(2)

The ^1H NMR spectrum of a quasi square-pyramidal complex *cis*-$[PtCl(PEt_3)_2(phen)]BF_4$[21] showed that the two halves of phen are environmentally averaged in solution even at −80 °C.[22] The mechanism of the fluxional motion can not be dissociative, since couplings between Pt and both P and α-H of phen are retained in the fast-exchange limit NMR spectra. The ^{31}P NMR spectra also certified retention of the mutually cis arrangement of the PEt_3 ligands. All these findings are consistent with mechanism (2).[22] The fluxional process by which the metal changes its point of attachment to the α-diimine ligand in some *trans*-$[MCl_2L(dim)]$ complexes (M=Pd, Pt; L=unidentate tertiary phosphine or arsine) was also interpreted based on the same mechanism, that is oscillatory motion of the chelated α-diimine in a five-coordinate square-pyramidal intermediate.[23]

The observed ^{19}F NMR spectra of **1a** in Fig. 5 are rationalized if the Pd^{II} complex undergoes both modes of intramolecular rearrangement (Eqs. 1 and 2) concurrently. Alternatively, either one of the twist motions analogous to those proposed by Ray and Dutt, Bailar, and Springer and Sievers as the intramolecular mechanism for racemization of octahedral complexes[24] will also be effective for averaging environments of some fluorine atoms in **1a**. For example Eq. 3 shows the Ray-Dutt twist, in which the (O_{c1}, O_t) chelate ring rotates by 90 ° on the basal plane and the (O_a, O_{c2}) chelate ring moves synchronously on the plane perpendicular to the P-M axis.

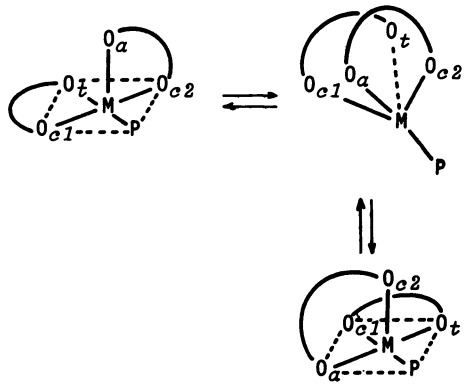

(3)

It should be noted that mechanism (3) does not exchange the basal and apical hfac ligands although both halves of each hfac are averaged. Therefore it is only supplementary to mechanism(1) in averaging all four CF_3 groups.

After we had completed this investigation,[6] Siedle and his collaborators[17] reported the X-ray structure of $[Pd(hfac)_2(PPh_3)]$ which is quite similar to that of **1a** and analyzed the dynamic ^{19}F NMR spectra of **1a** in CD_2Cl_2 to obtain the activation parameters, $\Delta H^{\ddagger}$= 7.7 ±1 kcal mol^{-1} and $\Delta S^{\ddagger}$=−20±5 cal deg^{-1} mol^{-1} (1 cal=4.184 J). They preferred a transition state of the square-pyramidal structure with the phosphine ligand at the apical position which makes all CF_3 groups equivalent. However, this symmetrical transition state may need a much higher activation energy, since the five-coordinate $Pd^{II}$and Pt^{II} complexes cited above have the strongly-bonding ligands such as tertiary phosphines and the cyanide ion exclusively at the basal positions. Figure 5 clearly indicates that four CF_3 groups are averaged not simultaneously by a single process, but by two consecutive processes at least in the case of Pt^{II} complex **2a**. Wernberg and Hazell[15] found that $[PtCN(phen)_2]^+$ has a square-

pyramidal structure in the solid state with one of the phenanthroline nitrogens at the apical position, but its ^{13}C NMR spectrum showed no difference between the two phen ligands and furthermore both halves of each chelating molecule gave identical signals. They proposed the intramolecular transformation processes *via* trigonal bipyramids, denying a square-pyramidal transition state with the cyanide at the apical position because of the steric hindrance between the two phen molecules on the basal plane.[15]

^{13}C NMR Spectra: Table 8 lists the ^{13}C NMR data. Complex **1a** shows one set of signals. On the other hand, **2a**, **2b**, and **2g** exhibit two sets of signals from the CF_3 and CO carbons, although the CH signal is single in each case. These spectral features are quite similar to those observed for ^{1}H and ^{19}F NMR spectra and rationalized by mechanism (1) for the Pt^{II} complexes and combined (1) and (2) for the Pd^{II} complexes. The carbonyl-carbon signals from **2g** in $CDCl_3$ are composed of two quartets, of which only the higher-field set couples to platinum (^2J(Pt-C)=16 Hz) and is assigned to the two CO carbons positioned cis to the phosphine. The CF_3 carbons also exhibit two sets of signals. One is a quartet flanked by the ^{195}Pt satellites (J(Pt-C)=89 Hz) and assigned to the CF_3 groups positioned cis to the phosphine. The other is a doublet of quartets coupling to ^{31}P and is considered to be an averaged signal from the CF_3 groups at the trans and apical sites, of which the ^{195}Pt satellites are indiscernible.

The ^{13}C NMR spectrum of **2g** in C_6D_6 at room temperature is quite similar to that in $CDCl_3$, but the CF_3 carbon signal at 80 °C appears as a single doublet of quartets, indicating that environments of all four CF_3 groups are averaged at this temperature. The ^1J(F-C) (286 Hz) and ^4J(P-C) (2 Hz) values are also averaged. The fluxional motion is rapid at room temperature for all Pd^{II} complexes and [Pt(hfac)$_2$(PPh$_3$)] (**2c**), the averaged ^1J(C-F) value being 286 Hz in either case. The rate of fluxional motion decreases with increasing bulkiness of tertiary phosphines in the sequence $PPh_3 > PCy_3 > P(o\text{-tolyl})_3$. The ^{195}Pt NMR signal from **2a** in $CDCl_3$ was recorded as a doublet at 295.7 ppm upfield from external $K_2[PtCl_4]$, ^1J(Pt-P) being 448_5 Hz.

^{31}P NMR Spectra: The ^{31}P{^{1}H} NMR data are collected in Table 9. The ^1J(Pt-P) values are rather large lying in the range of 4130—4540 Hz. The δ_P and

Table 8. ^{13}C NMR Data for [M(hfac)$_2$L] at 30 °C[a]

Compd	Solvent	hfac			L	
		CF_3	CH	CO	Me	Ph
1a	$CDCl_3$	116.6q [286]	89.5 (165)	174.0q [34]	23.0 (127)((7))	C^1 121.9d((60)), C^2 143.0d((9)), C^3 132.2d(161)((9)), C^4 132.3d(164)((3)), C^5 126.2d(164)((13)), C^6 135.4d(162)((13))
2a	$CDCl_3$	116.3q [283]{90} 116.8dq [288]((5))	91.7 (164){44}	174.3q [34]{b} 169.4q [34]	22.7d (127)((6))	C^1 121.6d((66)){19}, C^2 142.9d((9)){19} C^3 132.2d(164)((12)), C^4 132.0d(164)((2)) C^5 125.9d(164)((12)), C^6 135.5d(168)((13)){21}
2b	CD_2Cl_2	b)	92.4 {45}	174.7 [34]{b} 170.1 [36]		
1c	$CDCl_3$	116.7dq [286]((3))	89.5 (164)	174.3q [34]		C^1 124.4d((58)), C^2,C^6 134.2d(164)((11)) C^3,C^5 128.9d(161)((12)), C^4 132.2d(163)((3))
2c	CD_2Cl_2	117.1dq [286]((2))	92.2 {45}	172br		C^1 125.2d((68)){27}, C^2,C^6 134.4d((11)){21} C^3,C^5 129.0d((12)), C^4 132.3d((3))
2e	$CDCl_3$	b)	92.3 {51}	b)	9.8d ((45)){29}	b)
2f	$CDCl_3$	117.0q [286]	92.2 {63}	174.7q {33}	Et: CH_3 6.8d((3)){21}, CH_2 13.2d((39)){31}	
1g	$CDCl_3$	117.0dq [286]((3))	89.5 (164)	174.1q [34]		Cy: C^1 31.7d((24)), C^2,C^6 27.3d((12)) C^3,C^5 28.4d((3)), C^4 26.1d((2))
2g	$CDCl_3$	117.1q [284]{89} 117.1dq [288]((4))	91.5 {44}	169.4q [34]{16} 174.5q [35]		Cy: C^1 30.5d((32)){24}, C^2,C^6 27.3d((12)) C^3,C^5 28.3d((2)){17}, C^4 26.3d((2))
	C_6D_6	117.6q [284]{b} 117.6dq [288]((4))	92.0 (163){44}	169.6q [34]{18} 176.3q [35]		Cy: C^1 30.6d(b)((33)){24}, C^2, C^6 27.5d(b)((11)) C^3,C^5 28.5d(b)((3)){20}, C^4 26.4d(b)((2))
	C_6D_6[c]	117.8dq [286]((2))	92.4 {43}	173br		Cy: C^1 31.2d((32)){25}, C^2,C^6 27.6d((12)) C^3,C^5 28.8d((3)){18}, C^4 26.5d((2))
1j	$CDCl_3$	116.4q [286]	89.8	174.3q [33]		C^1 126.8, C^2,C^6 133.3, C^3,C^5 129.5, C^4 131.7

a) Chemical shifts in ppm from internal Me_4Si. Figures in parentheses, double parentheses, braces, and brankets are ^1J(C-H), J(P-C), J(Pt-C), and J(F-C) in Hz, respectively. d=Doublet, q=quartet. b) Indiscernible. c) At 80 °C.

Table 9. $^{31}P\{^1H\}$ NMR data for $[M(hfac)_2(PR_3)]$[a)]

Compd	Solvent	Temp °C	δ_P ppm	^1J(Pt-P) Hz
1a	CD_2Cl_2	30	18.7	
		−50	18.0	
2a	CD_2Cl_2	30	−7.4	447_4
		−50	−8.2	442_2
1c	CD_2Cl_2	30	20.9	
		−50	21.4	
2c	CD_2CL_2	30	−4.6	454_1
		−50	−4.1	448_0
2e	$CDCl_3$	30	−22.9	437_2
2f	$CDCl_3$	30	2.7	425_3
1g	$CDCl_3$	30	45.5	
		−30	46.3	
2g	$CDCl_3$	30	12.6	418_4
		−30	13.2	413_4

a) Chemical shifts (δ_P) in ppm from external H_3PO_4 at 30 °C (downfield positive).

^1J(Pt-P) values show no appreciable change with temperature in the −50 to +30 °C region, indicating retention of the five-coordinate structure. When an equimolar amount of PMe_2Ph or PEt_3 was added to $[Pt(hfac)_2]$ in $CDCl_3$, signals assignable to $[Pt(hfac)(PR_3)_2](hfac)$ appeared besides those from **2e** and **2f**, respectively, and increased with time in the expense of the latters. The disproportionation reactions of **2e** and **2f** to produce $[Pt(hfac)(PR_3)_2](hfac)$ and $[Pt(hfac)_2]$ were completed in about 2 d. The tertiary phosphines in the square-planar complexes $[Pt(hfac)(PR_3)_2](hfac)$ give the ^{31}P NMR signals in the 5—10 ppm lower field than those in the corresponding five-coordinate complexes and their ^1J(Pt-P) values are appreciably lower lying in the region of 3670—4020 Hz. On the other hand, $[Pd(hfac)_2]$ reacts with equimolar amounts of PMe_2Ph and PEt_3 rapidly with heat evolution to afford $[Pd(hfac)(PR_3)_2](hfac)$ exclusively. NMR signals assignable to the five-coordinate complexes were not detected.

When an equimolar amount of PPh_3 is added to $[M(hfac)_2]$ (M=Pd and Pt) and PCy_3 to $[Pd(hfac)_2]$ in CD_2Cl_2, complexes **1c**, **2c**, and **1g** are formed in equilibrium with small amounts of the $[M(hfac)(PR_3)_2](hfac)$-type complexes, respectively. (In the case of **1c**, signals attributable to $[Pd(hfac)(hfac\text{-}C^3)(PPh_3)]$ are also observed.) When another equivalent of phosphines is added to the solution, only the signals from $[M(hfac)(PR_3)_2](hfac)$ are observed. On the other hand, complexes **1a**, **2a**, and **2g** are quite stable in $CDCl_3$ and do not react with excess amounts of phosphines. These observations indicate that the thermodynamic stability of the five-coordinate complex becomes higher with increase in the bulkiness (cone angle[25)]) of tertiary phosphine in the sequence $PPhMe_2 \approx PEt_3 < PPh_3 < PCy_3 < P(o\text{-tolyl})_3$. Difference in behaviors of **1g** and **2g** suggests that the stability of the five-coordinate complex is higher for platinum(II) than for palladium(II).

We wish to thank Mr. Junichi Gohda and Dr. Isamu Kinoshita for elemental analysis and measurements of electronic spectra at low temperatures, respectively. We also are grateful to Mr. Tetsu Hinomoto of JEOL, Ltd. for measurements of the ^{19}F and ^{195}Pt NMR spectra.

References

1) a) S. Okeya, H. Sazaki, M. Ogita, T. Takemoto, Y. Onuki, Y. Nakamura, B. K. Mohapatra, and S. Kawaguchi, *Bull. Chem. Soc. Jpn.*, **54**, 1978 (1981); b) S. Okeya, H. Yoshimatsu, Y. Nakamura, and S. Kawaguchi, *ibid.*, **55**, 483 (1982); c) S. Okeya, Y. Nakamura, and S. Kawaguchi, *ibid.*, **55**, 1460 (1982).
2) S. Okeya, Y. Nakamura, and S. Kawaguchi, *Bull. Chem. Soc. Jpn.*, **54**, 3396 (1981).
3) F. Basolo and R. G. Pearson, "Mechanisms of Inorganic Reactions," 2nd ed, Wiley, New York (1967), p. 351; L. Cattalini, *Progr. Inorg. Chem.*, **13**, 263 (1970).
4) In the reaction of $RhCl\{Sb(p\text{-tolyl})_3\}$(1,5-cyclooctadiene) with nitrogen bases, the five-coordinate intermediate is exceptionally stable and detected spectroscopically: L. Cattalini, R. Ugo, and A. Orio, *J. Am. Chem. Soc.*, **90**, 4800 (1968).
5) S. Matsumoto and S. Kawaguchi, *Bull. Chem. Soc. Jpn.*, **54**, 1704 (1981).
6) S. Okeya, T. Miyamoto, S. Ooi, Y. Nakamura, and S. Kawaguchi, *Inorg. Chim. Acta*, **45**, L135 (1980).
7) S. Okeya, S. Ooi, K. Matsumoto, Y. Nakamura, and S. Kawaguchi, *Bull. Chem. Soc. Jpn.*, **54**, 1085 (1981); S. Okeya and S. Kawaguchi, *Inorg. Synth.*, **20**, 65 (1980).
8) L. K. Templeton and D. H. Templeton, Abstracts, American Crystallographic Association Proceedings (1973), Series 2, Vol. 1.
9) "International Tables for X-Ray Crystallography," Kynoch Press, Birmingham, (1974), Vol. IV.
10) "UNICS," The Crystallographic Society of Japan (1969).
11) C. K. Johnson, ORTEP II, Report ORNL-5138, Oak Ridge National Laboratory, Oak Ridge, TN (1976).
12) K. M. Chui and H. M. Powell, *J. Chem. Soc., Dalton Trans.*, **1974**, 1879.
13) K. M. Chui and H. M. Powell, *J. Chem. Soc., Dalton Trans.*, **1974**, 2117.
14) W. J. Louw, D. J. A. de Waal, and G. J. Kruger, *J. Chem. Soc., Dalton Trans.*, **1976**, 2364.
15) O. Wernberg and A. Hazell, *J. Chem. Soc., Dalton Trans.*, **1980**, 973.
16) A. R. Siedle, R. A. Newmark, and L. H. Pignolet, *J. Am. Chem. Soc.*, **103**, 4947 (1981).
17) A. R. Siedle, R. A. Newmark, and L. H. Pignolet, *J. Am. Chem. Soc.*, **104**, 6584 (1982).
18) S. Ooi, T. Matsushita, K. Nishimoto, S. Okeya, Y. Nakamura, and S. Kawaguchi, *Bull. Chem. Soc. Jpn.*, **56**, 3297 (1983).
19) For example, A. Musco, W. Kuran, A. Silvani, and M. W. Anker, *J. Chem. Soc., Chem. Commun.*, **1973**, 938; W. Kuran and A. Musco, *Inorg. Chim. Acta*, **12**, 187 (1975); S. Otsuka, T. Yoshida, M. Matsumoto, and K. Nakatsu, *J. Am. Chem. Soc.*, **98**, 5850 (1976); Z. Dawoodi, M. L. H. Green, V. S. B. Mtetwa, and K. Prout, *J. Chem. Soc., Chem. Commun.*, **1982**, 802, 1410.
20) For example, G. L. Geoffroy and R. Pierantozzi, *J. Am. Chem. Soc.*, **98**, 8054 (1976); E. L. Muetterties, *Chem. Soc. Rev.*, **11**, 283 (1982).
21) G. W. Bushnell, K. R. Dixon, and M. A. Khan, *Can. J. Chem.*, **52**, 1367 (1974).
22) K. R. Dixon, *Inorg. Chem.*, **16**, 2618 (1977).
23) H. van der Poel, G. van Koten, and K. Vrieze, *Inorg. Chem.*, **19**, 1145 (1980).
24) C. S. Springer, Jr. and R. E. Sievers, *Inorg. Chem.*, **6**, 852 (1967).
25) C. A. Tolman, *Chem. Rev.*, **77**, 313 (1977).